CHAPTER V

THERMAL PROPERTIES AND VIBRATIONAL STUDIES OF BOROPHOSPHATE GLASSES

ABSTRACT

This chapter deals with the thermal properties and vibrational studies of copper doped borophosphate glasses. Thermal properties are studied using thermo gravimetric experimental techniques. The vibrational studies of glass systems are studied using Fourier Transform Infrared Spectroscopic techniques. From the thermal properties, we obtained the stability of the glass materials and from the vibrational studies, vibration of NBO's were studied.

RESULTS AND DISCUSSION

5.1 Thermal Analysis using Thermogravimetry (TG) and Differential Thermal Analysis (DTA)

Thermal analysis is defined as a group of techniques in which a physical property of a substance and or its reaction products is measured as a function of temperature while the substance is subjected to a controlled temperature program. These methods include Thermogravimetry (TG) and Differential Thermal Analysis (DTA).

The TGA/DTA analysis of pure and CuO doped glass samples are shown in the Figs. 5.1.1. – 5.1.4. The decomposition pattern has been formulated to account for the weight losses observed and shown in Table 5.1.1. Both pure and doped samples exhibit a different stage of decomposition with producing detectable weight loss dependent intermediate species.

In the present work, DTA technique has been employed to determine glass transition temperature (T_g), glass crystallization temperature (T_c), glass melting temperature (T_m) and to tell the possibility of formation of crystallization and phase separation in borate glasses [1]. The glass transition temperature depends on the strength and connectivity of the network [2]. It is clear from Table 5.1.1. that the strength and connectivity of the network increases with increase of CuO content. The increase of T_g with CuO content also suggest a continuous change of the glass matrix [3, 4].

From the TGA (Fig. 5.1.1.) total 3.34% weight reduction which can be divided in to 3 main weight losses between 80-190 °C (1.06%), 300-420 °C (1.02%) and 500-700 °C (1.26%) for pure sample S_0. The weight loss with first step corresponds to release to water in the sample at 100 °C, while the 2^{nd} and 3^{rd} steps correspond to the decomposition of the sample.

For doped samples, 1.93 % weight reduction was observed for sample S_4 (CuO – 0.2 mol%) (Fig. 5.1.2.), 1.64% weight reduction for sample S_5 (CuO – 0.25 mol%) (Fig. 5.1.3.) and the observed weight reduction was 1.28% for sample S_{10} (CuO - 0.5 mol%), respectively.

From the DTA curve, two endothermic peaks appear for the pure samples. The low temperature endothermic peak at around T_{g_1} = 356.4 °C, due to the decomposition of the samples. This endothermic peak is followed by an exothermic peak beginning at T_{c_1} = 611.4 °C. The exothermic peak is probably due to a reaction involving the crystallization of calcite. Finally melting takes place in the range of 700-1100 °C. The endothermic peak T_{M_1} =766.4 °C may be attributed to the melting of the sample.

For doped sample (Fig.5.1.3. – S_4 – CuO – 0.2%) both the glass transition and crystallization temperature are shifted to higher temperature T_{g_2} = 366.4 °C and T_{c_2} = 631.4 °C, respectively . Further in doped glass the melting is not sharp and a broad endothermic peak at T_{M_2} = 901.4 °C is obtained. The decrease in the sharpness of the peak suggests that CuO doped glass is more amorphous. The higher T_g values of the doped glass suggest an increase in the cross link density, which improves its chemical durability. In the presence of 0.25 wt% CuO (Fig. 5.1.4.) the glass transition is shifted to lower temperatures T_{g_3} = 346.4°C and increase in glass crystallization temperature T_{c_3} = 661.4 °C. Decrease in T_g may be due to the higher cross- link density of cation is replaced by a cation of lower cross- link density of the sample [5, 6, 7]. It is believed that T_g depends on the strength of chemical bonds in the structure.

Table 5.1.1. Glass Transition(T_g), Crystallization(T_c) and Melting(T_m) Temperatures of Pure and CuO doped Borate Glasses

Temperature (^oC)	S_0	S_4	S_5	S_{10}
T_g	356.4	366.4	346.4	606.4
T_c	611.4	631.4	661.4	671.4
T_m	766.4	901.4	911.4	941.4

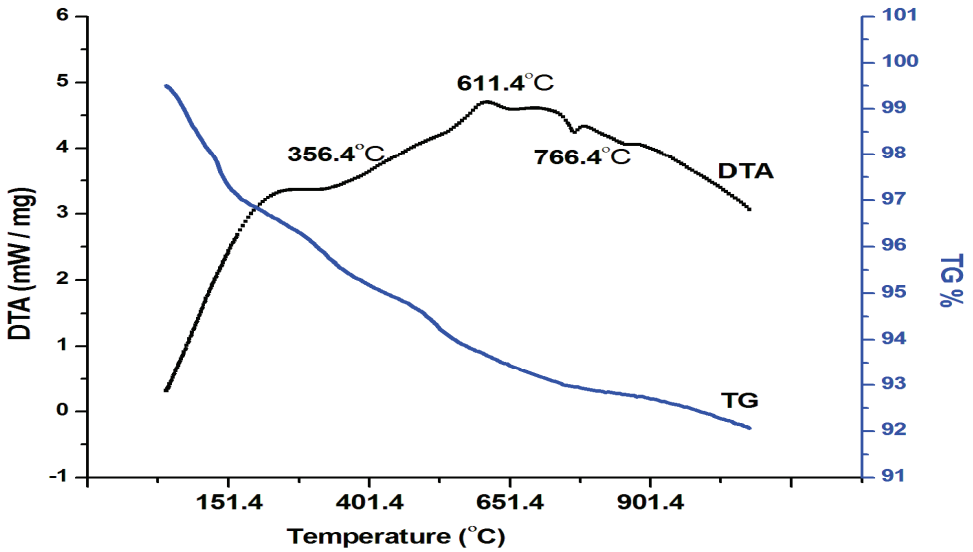

Fig. 5.1.1. TG-DTA graph of NCPB (S_0 – pure) glass

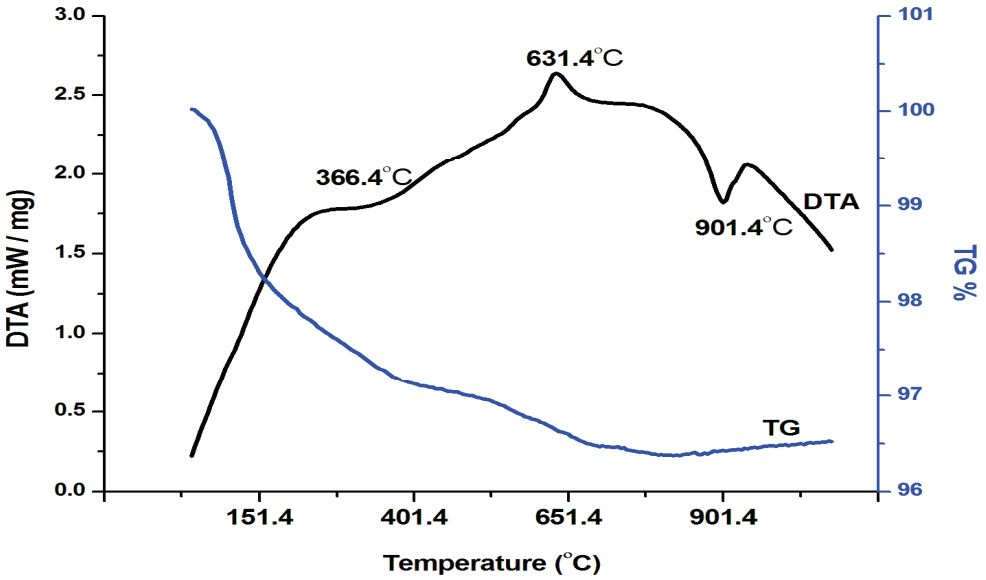

Fig. 5.1.2. TG-DTA graph of NCPBC (S_4 – CuO 0.2) glass

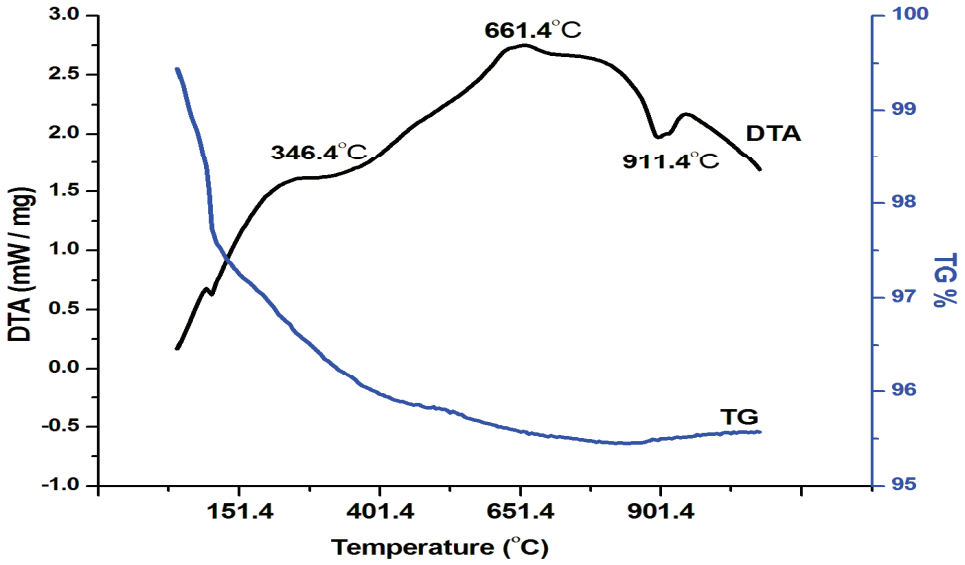

Fig. 5.1.3. TG-DTA graph of NCPBC (S_5 – CuO 0.25) glass

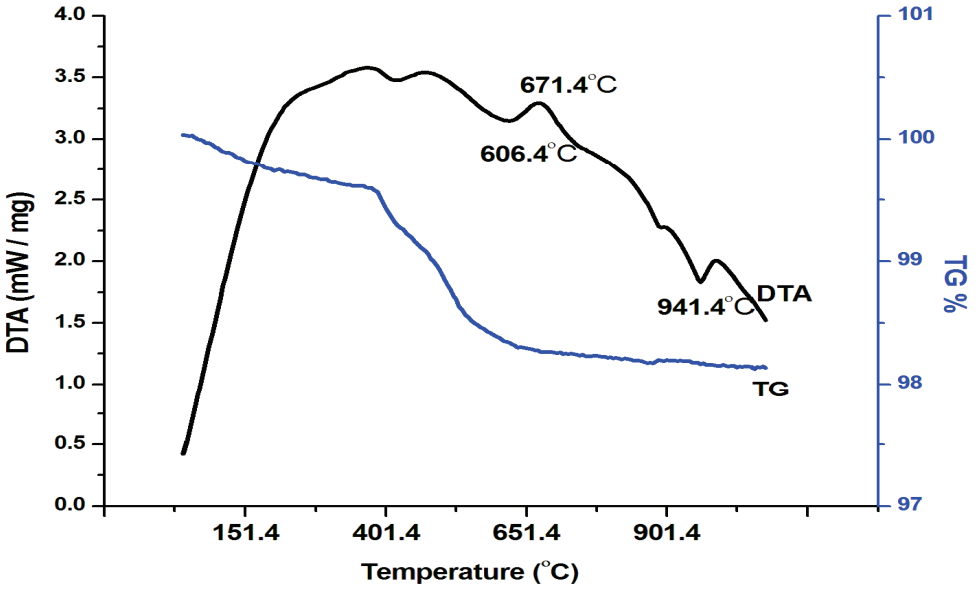

Fig. 5.1.4. TG-DTA graph of NCPBC (S_{10} – CuO 0.5) glass

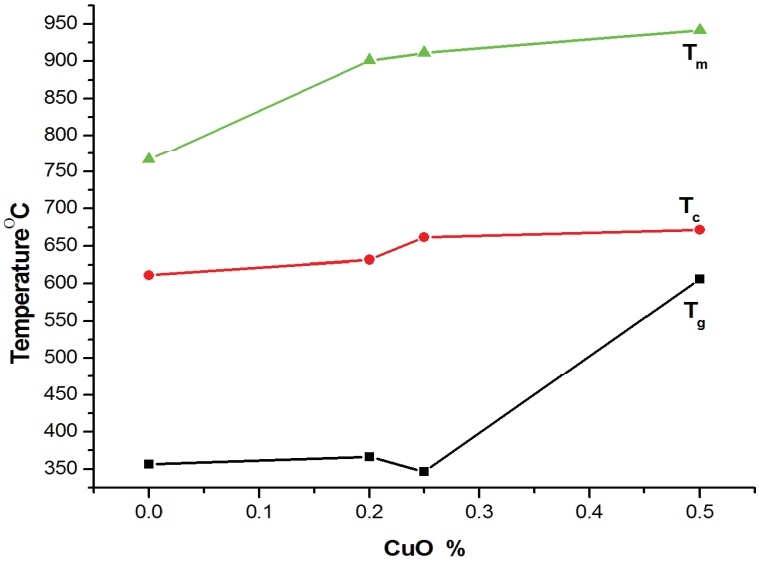

Fig. 5.1.5. Compositional dependency of glass transition, crystallization and melting temperature

TMI in general, plays the role of network modifier and non-bridging oxygen increases with increase of TMI content in the glass system. Increase of NBO indicated the breaking of chemical bond, which in turn decrease of T_g [8]. Endothermic peak at T_{M_3} = 911.4 °C is noticed.

From the Fig. 5.1.4 for sample S_{10} (5.0 wt% CuO), both the glass transition and crystallization temperature are increased to T_{g_4} = 606.4 °C and T_{c_4} = 671.4 °C respectively. Glass melting temperature T_{M_4} = 941.4 °C is noticed. The observed increase in Tg for glasses is due to the destruction of non- bridging oxygen atoms (NBO) [7, 9].

Thermal study of the glasses were performed because any change in the coordination number of network forming atoms, or the formation of non-bridging oxygen, is known to be reflected in the T_g. Fig. 5.1.5 illustrates the variation of T_g, T_c and T_m with compositions. A maximum in the T_g vs. CuO content curve is also reported [10]. It is believed that T_g is depend on the strength of chemical bonds in the structure. TMI in general, plays the role of a network modifier and non-bridging oxygen increases with the increase of TMI content in the glass system. Increase of non-bridging oxygen indicates the breaking of chemical bonds, which in turn decrease the T_g. Increase of T_g from 356.4 °C to 606.4 °C with the increase of TMI, indicates the increase of strength and connectivity of the glass structure in this case.

The results indicate the increase of strength and connectivity of the glass structure.

5.2. Molecular Vibration study using Fourier Transform Infrared (FTIR) Spectroscopy

The FTIR spectroscopy is one of the powerful techniques used for molecular characterization. The FTIR spectrum contains both elemental and structural information and can be considered as a definite fingerprint of the constituents of the samples.

FT-IR spectra were recorded using Perkin Elmer Model No, C-92107 available at the Department of Physics, Manonmaniam Sundaranar University, in the range of 4000 – 400 cm^{-1} with a resolution ± 4 cm^{-1}.

The following information is required for structural analysis of oxide glasses[11].

i. Type of the bridging bonds of oxygen, which link the coordination polyhedra of the framework and the composition of chemical inhomogeneities in the structure of glass.

ii. The coordination number of the compound with respect to oxygen, especially of network formers.

iii. The change in oxygen bonds of the framework induced by the cation modifiers which combine with those bonds. In general, IR analysis of absorption of the borate glasses are very high in the region of wavenumbers less than 2000 cm^{-1}.

In the infrared spectral region, the vibrational modes of the borate network have four distinct frequency region [12, 13].

a. The first group of bands, which occur at 1200-1600 cm^{-1} is due to the asymmetric stretching vibration of the B-O bonds in BO_3 units. The region between 1150-1400 cm^{-1} is characteristic of vibrations of non-bridging PO_2 groups.

b. The second group lies between 800 and 1200 cm^{-1} and is due to the B-O stretching of the tetrahedral BO_4 units. The region around 900-1150 cm^{-1} is characteristic of terminal $P\text{-}O^-$ and PO_3 groups.

c. The third group is observed around 700 cm^{-1} and is due to the bending of B-O-B linkages in the borate network. Deformation modes of both types of units are active between 600 and 800 cm^{-1} . The region between 700-900 cm^{-1} is characteristic of vibrations of bridging P-O-P groups. [14,15].

In the present glass system, predominantly 7 bands are observed as shown in Figs. 5.2.1 to 5.2.4 and also summarized in the Tables 5.2.1 - 5.1.3.

Table 5.2.1. Observed FT-IR band positions of Pure NCPB glass and CuO doped NCPBC glasses

Glasses											Band Assignments	References
S_0 (Pure)	S_1	S_2	S_3	S_4	S_5	S_6	S_7	S_8	S_9	S_{10}		
Wave Number (cm^{-1})												
1326	1321	1318	1306	1398 1309	1312	1400	1407	1403	-	-	Symmetric stretching of B-O bond Asymmetric stretching modes of PO_2	M.S. Gaafar. et. al. J.Alloys & Compounds 475 (2009) 535-542. G. Rama Sundari et.al. J.Non-Crys.Solids. 365 (2013) 6-12. Sunil Thomas et.al. J.Non-Crys.Solids. 376 (2013) 106-116. M. Ganguli, J.Phys.Chem. B 103 (1999) 920-930. Razvan.Stefan et.al. J.Non-Crys.Solids. 358 (2012) 839-846.
-	-	-	-	-	-	-	-	-	1268	1255	B –O stretching vibrations Asymmetric stretching modes of PO_2	T.G.V.M.Rao et.al. J.Alloys & Compounds 557 (2013) 209-217.

Table 5.2.2. Observed FT-IR band positions of Pure NCPB glass and CuO doped NCPBC glasses

Glasses											Band Assignments	References
S_0 (Pure)	S_1	S_2	S_3	S_4	S_5	S_6	S_7	S_8	S_9	S_{10}		
Wave Number (cm^{-1})												
1030	1013	1016	1031	1016	1010	1020	1028	1020	1014	1002	Combined vibrations of borate groups Vibration of PO_3 groups (chain end groups)	T.G.V.M.Rao et.al. J.Alloys & Compounds 557 (2013) 209-217. P. Pascuta et.al., J.Matel.Sci.Matter Electron 21 (2010) 338.
869	876	859	859	861	856	859	859	861	859	878	Stretching vibrations of NBOs in BO_4 units. Asymmetric stretching of P-O-P groups	T.G.V.M.Rao et.al. J.Alloys & Compounds 557 (2013) 209-217. P. Pascuta et.al., J.Matel.Sci.Matter Electron 21 (2010) 338.
723	729	725	722	720	722	721	731	714 636	715	721	Bending relaxation of B-O Symmetric stretching of P-O-P groups	Razvan.Stefan et.al. J.Non-Crys.Solids. 358 (2012) 839-846. A. Chahine et.al. Mat.Letters. 58 (2004) 2776-2780 & D.Carta et.al., J.Non- Cry. Solids., 535 (2007) 1141-1149.

Table 5.2.3. Observed FT-IR band positions of Pure NCPB glass and CuO doped NCPBC glasses

Glasses											Band Assignments	References
S_0 (Pure)	S_1	S_2	S_3	S_4	S_5	S_6	S_7	S_8	S_9	S_{10}		
Wave Number (cm^{-1})												
573	580	560	562	561	563	535	554	567 537	566	571	B-O-B stretching vibrations Stretching vibration of P=O and P-O bonds.	W.B. With et.al. Borate Glasses: Structure, properties, Application, Plenum, Newyork, (1978). Gurbinder Kaur et.al. J.Non-Crys.Solids. 358 (2012) 2589-2596. K. Zheng et.al. J.Non-Crys.Solids, 358 (2012) 387-391.
511	489	497	488	509	487	498	502	507	494	506	Absorption due to $(PO_4)^{3-}$	Razvan.Stefan et.al. J.Non-Crys.Solids. 358 (2012) 839-846.

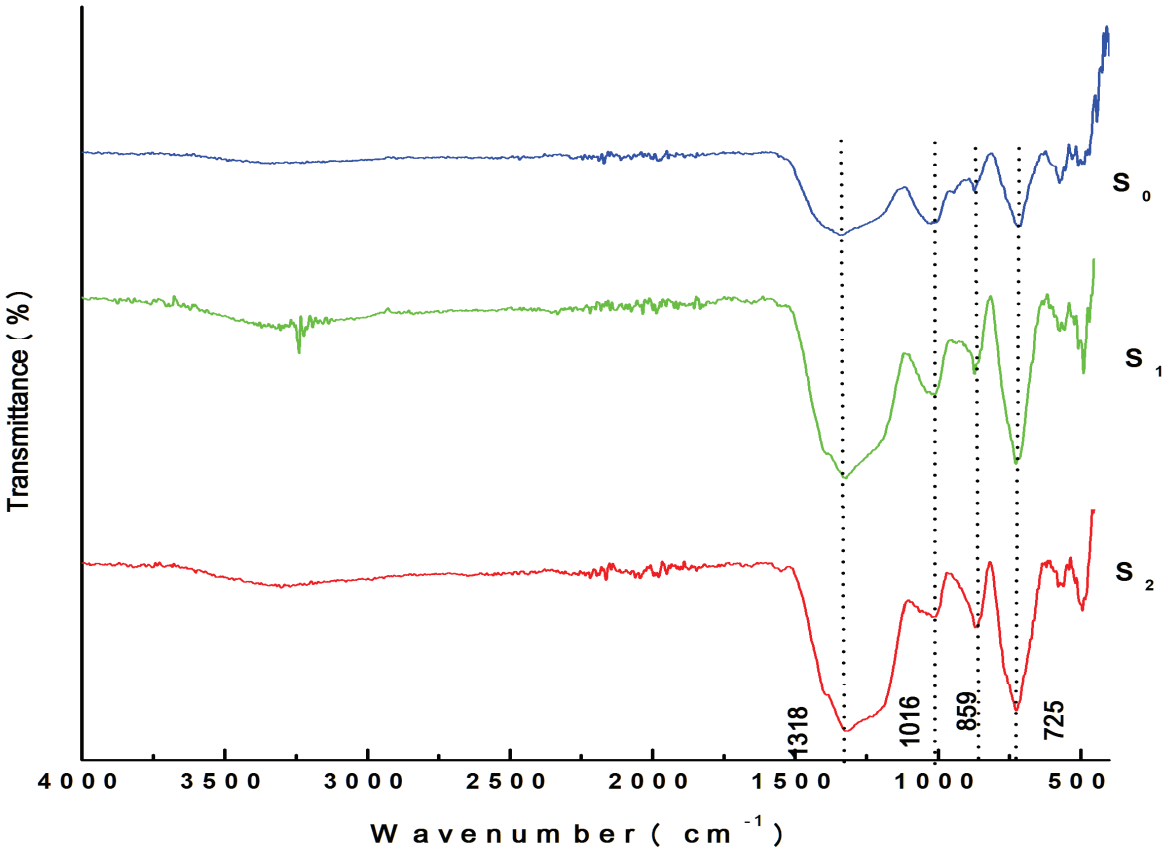

Fig. 5.2.1. FT-IR Spectra of Pure NCPB glass (S_0) and 0.05 to 0.1 CuO doped NCPBC glasses ($S_1 – S_2$)

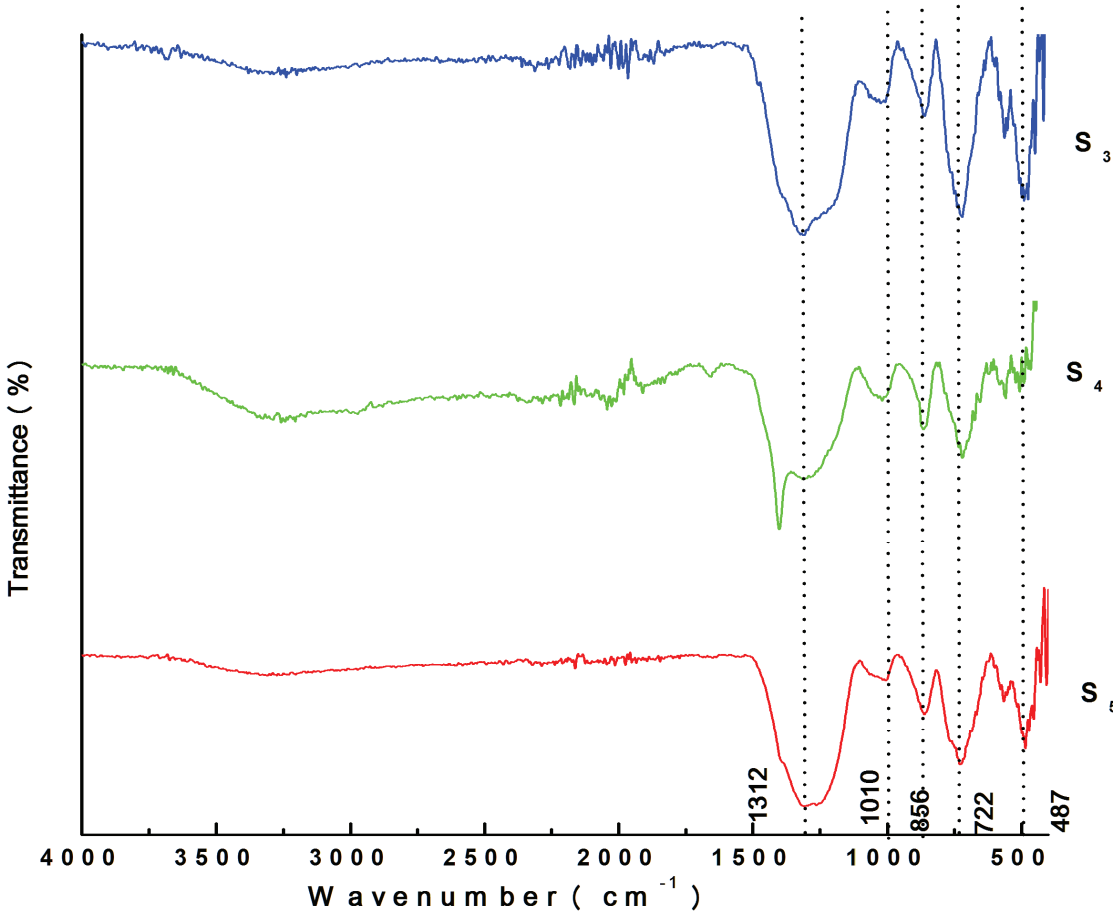

Fig. 5.2.2. FT-IR Spectra of 0.15 to 0.25 CuO doped NCPBC glasses (S_3 – S_5)

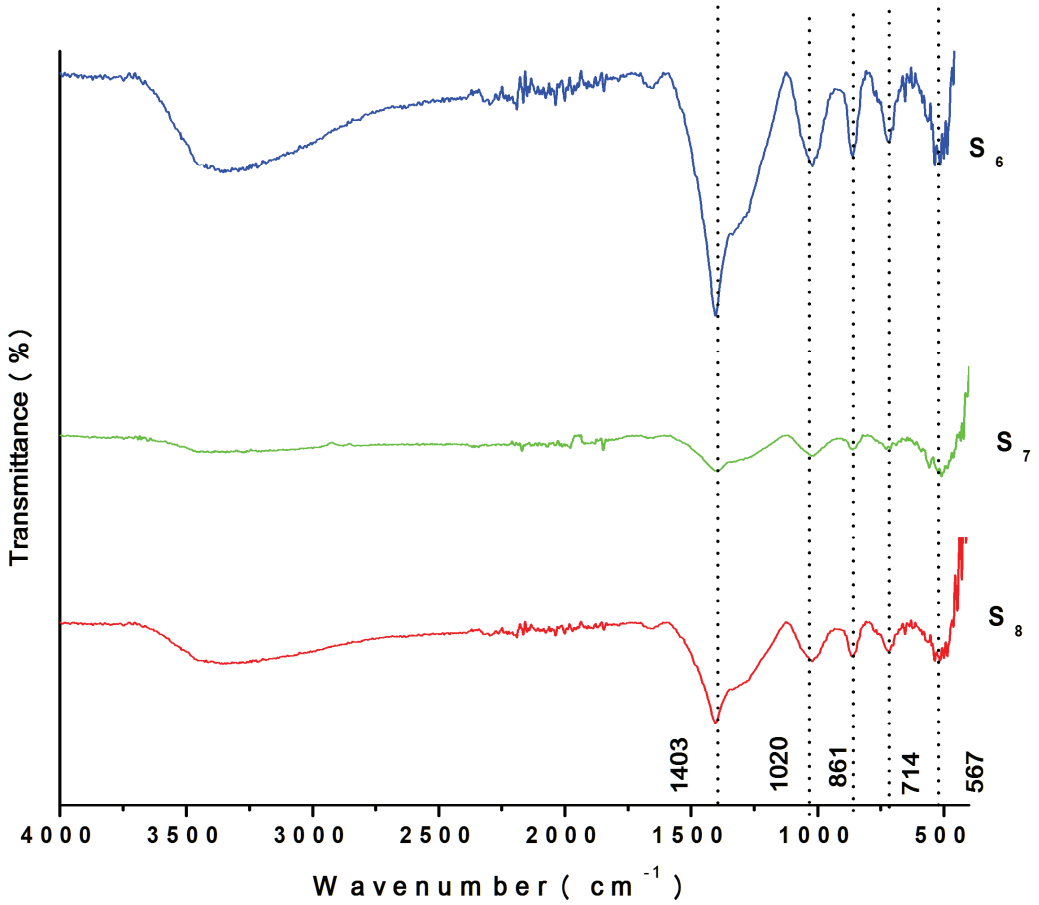

Fig. 5.2.3. FT-IR Spectra of 0.3 to 0.4 CuO doped NCPBC glasses (S_6 – S_8)

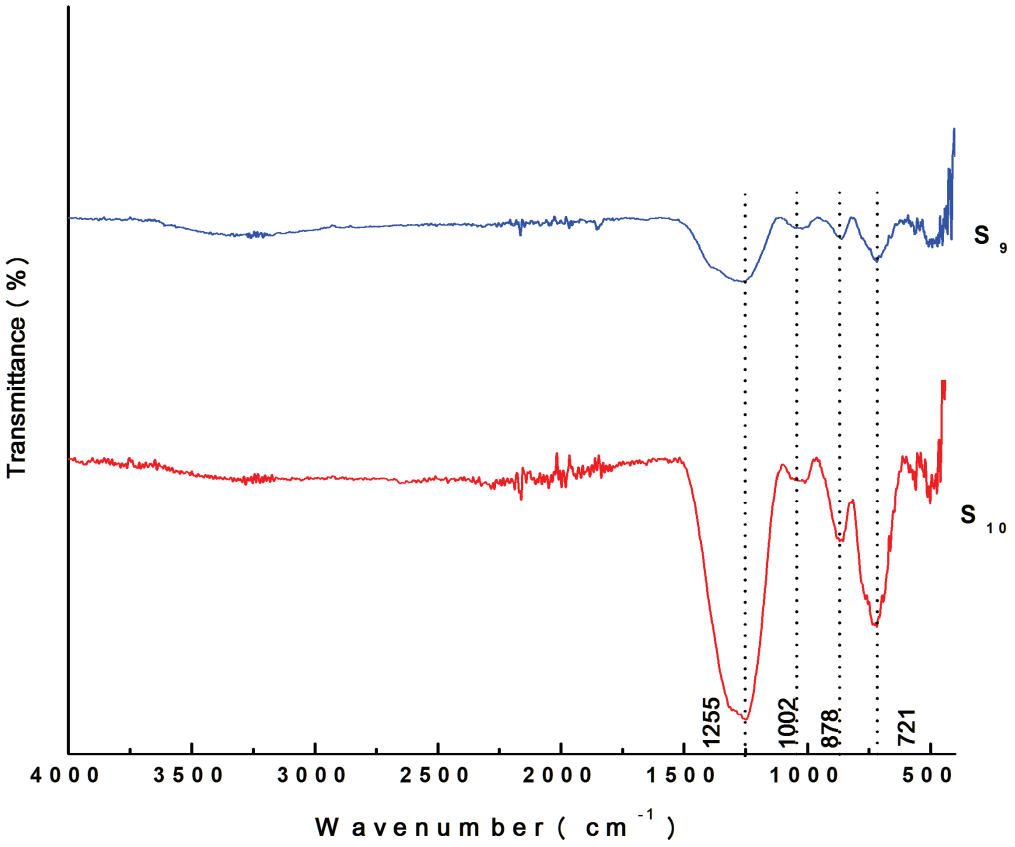

Fig. 5.2.4. FT-IR Spectra of 0.45 to 0.5 CuO doped NCPBC glasses (S_9 – S_{10})

The relatively sharper FTIR peaks of glass samples can be due to strong vibrational frequency of the various groups present in the glasses. The small shifting of FTIR peaks to the lower wave number side (1326 to 1268 cm^{-1}, 878 to 731 cm^{-1} , 731 to 571 cm^{-1} & 571 to 501 cm^{-1}) is observed in glasses as the modifier changed.

The overall spectra consists of distinctive absorption peaks centered in the mid-region extending from 450 – 1500 cm^{-1} [16]. The peak at 450-550 cm^{-1} is due to $(PO_4)^{3-}$ units. The peak at 550-600 cm^{-1} is due to B-O-B stretching vibrations involving oxygen atoms outside borate rings [17]. The peak at 570 cm^{-1} can be attributed to stretching vibration of P=O and P-O bonds of the phosphate groups [18]. The peak at 650-750 cm^{-1} can be due to the bending relaxation of the B-O linkages in the borate network [19]. The peak at 720 cm^{-1} are assigned to symmetric stretching of the bridging oxygen atoms bonded to a phosphorus atom [15,20]. The peak around 859 cm^{-1} can be due to the stretching vibrations of NBOs in BO_4 units [21]. The peak at 880 cm-1 is assigned to asymmetric stretching of P-O-P groups [20]. The peak ~ 1016 cm^{-1} is due to the combined vibrations of different types of borate groups belonging to BO_4 units (Tri, tetra, Penta borate and diborate) [20, 21]. The peak around 1000 cm^{-1} is assigned to the vibration of PO_3 groups (chain end groups) [20].

The peak ~ 1250 cm^{-1} is due to B-O stretching relaxation of the $(BO_3)^{3-}$ units in meta, orthoborate chains. The peak ~ 1180 cm^{-1} is assigned to symmetric stretching vibration of PO_2 groups [20]. The peak ~ 1320 cm^{-1} is due to asymmetric stretching relaxation of the B-O band of trigonal BO_3 units [22-25]. The peak at 1320 cm^{-1} is assigned to asymmetric stretching modes PO_2 of the non-bridging oxygen atoms bonded to the phosphorus atom [15]. The small peaks are occurring above 1500 cm^{-1}. These peaks are attributed to O-H bending that give rise to absorption in this region and the possibility of any absorbed water.

From the Figs. 5.2.1 to 5.2.4, it shows the absorption band of B-O asymmetric stretching mode shifts to lower frequencies as CuO content increases. We conclude that the addition of CuO does not affect the glasses, but a small shift in the B-O stretches mode towards the lower frequency.

The structural changes involved with the addition of CuO were analyzed based on the changes produced by the copper ions in the relative population of triangular and tetrahedral borate units and also the network modifier role in the studied glasses.

CONCLUSION

The TG-DTA results indicate a good thermal stability of the studied glasses. The FT-IR absorption spectra of CuO doped phosphate glasses provide information about the main characteristics frequencies for phosphate bonds present in the glass network such as P=O, P-O-P, O-P-O and P-O-H. The presence of P-O-H bond indicates the hygroscopic nature of these phosphate glasses. Addition of CuO in the glass matrix decreases the moisture content in the glass and increases the IR absorption. The FT-IR spectral analysis confirms the presence of absorption bands due to characteristic groups (BO_3, BO_4, PO_2, PO_3 and P=O) as the main glass consisting groups and also the vibration of NBOs.

REFERENCE

1. W. J. Gawandea, S. S. Yawale and S. P. Yawale, Vidarbha, *Journal of Science* 9(1), (**2014)** 11–17.
2. Ghosh, *Bull Mater Sci*, 18 (**1995**) 1 53.
3. S. Mandal, A. Ghosh , *Phys Rev., B*. 48 (**1993**) 9388.
4. A.El. Ghannam, E.Hamazawy, A.Yehia and J.Biomed, *J.Mater.Res.* 55, (**2001**) 387-395.
5. G.Upender, C. P. Vardhani, S.Suresh, A. M. Awasthi and V. Chandra mouli, *Mat. Chem. & Phy.,* 121, (**2010**) 335-341.
6. B. V. R. Chowdari and P. Pramoda kumara, *J. Non-Crys.Solids.,* 197, (**1996**) 31-40.
7. S. Saravanan, S. Rajesh and R. Palani, *Int.J. Recent Res. and Review*, Vol. VIII, Issue3, (**2015**).
8. Manisha Pal, Baishakhi Roy and Mrinal Pal, *J.Modern Phy*. 2 (**2011)** 1062 -1066.
9. M. Shapaan and F. M. Ebrahim, *Phy B.*, 405, (**2010**) 3217-3222.
10. P. Becker, *Crystal Research and Technology*, Vol. 38, No. 1, **(2003)** pp. 74-82.
11. N.A.Ghoneum E.I.Batal, H.A.Abdel Shafi and M.H.Azooz, *Proceedings of Egyptian conference of Chemistry* (**1996**) P.162.
12. A.A.Alemi, L.Kafi-Ahmadi, Sh.Karamipour Iranian, *J.Crystal & Minimum*. Vol.16 (**2009**) P.1387.
13. F.A.Khalifa, H.A.El-Batal, A.Azooz, *Ind.J.Pure & Appl.Phys*.36(6) (**1998**) pp. 314-318.
14. Daniela Carta, Jonathan C.Knowles, Mark E.Smith, Robert J.Newport*, J.Non-Crys.Solids* 353 (**2007)** 1141-1149.
15. Razvan.Stefan, Eugen Culea, Petru Pascutta, *J.Non-Crys.Solids*. 358 (**2012**) 839-846.

16. W.B.With, S.A.Brawer, T.Furukawa, G.J.Mc-Carty, L.D.Pye, V.D.Frechette (Eds)., *Borate Glasses: Structure, properties, Application,* Plenum, Newyork, (**1978)**.

17. Kai Zheng, Shengbing Yang, Jiaojiao Wang, Christian Russel, Changsheng Liu, Wen Liang, *J.Non-Crys.Solids*. 358 (**2012)** 387-391.

18. Gurbinder Kaur, O.P.Pandey, K.Singh, *J.Non-Crys.Solids*. 358 (**2012)** 2589-2596.

19. A.Chahine, M.Et-tabirou, J.L.Pascal, *Mat.Letters*, 58 (**2004)** 2776-2780.

20. T.G.V.M.Rao, A.Rajesh Kumar, K.Neeraja, N.Veeraiah, M.Rami Reddy, *J.Alloys & Compounds* 557 (**2013**) 209-217.

21. P.Pascuta, G.Bordi, E.Culea, *J.Matel.Sci.Matter Electron* 21 (**2010)** 338.

22. M.S.Gaafar. N.S.Abd El-Aal, O.W.Gerges, G.El-Amir, *J.Alloys & Compounds* 475 (**2009**) 535-542.

23. G.Rama Sundari, D.V.Sathish, T.Raghavendra Rao, Ch.Rama Krishna, Ch.Venkata Reddy, R.V.S.S.N.Ravikumar, *J.Non-Crys.Solids*. 365 (**2013)** 6-12.

24. Sunil Thomas, Sk.Nayab Rasool, M.Rathaiah, V.Venkatramu, Cyriac Joseph,N.V.Unnikrishnan*, J.Non-Crys.Solids*. 376 (**2013**) 106-116.

25. M.Ganguli, *J.Phys.Chem. B* 103 **(1999**) 920-930.